Free glycans derived from *O*-mannosylated glycoproteins suggest the presence of an *O*-glycoprotein degradation pathway in yeast

Received for publication, May 22, 2019, and in revised form, July 4, 2019 Published, Papers in Press, July 16, 2019, DOI 10.1074/jbc.RA119.009491

Hiroto Hirayama[‡], Tsugiyo Matsuda[‡], Yae Tsuchiya[‡], Ritsuko Oka[‡], Junichi Seino[‡], Chengcheng Huang[‡], Kazuki Nakajima[§], Yoichi Noda[¶], Yuichi Shichino[‖1], Shintaro Iwasaki[‖], and Tadashi Suzuki[‡2]**

*From the [‡]Glycometabolic Biochemistry Laboratory and the [‖]RNA Systems Biochemistry Laboratory, RIKEN Cluster for Pioneering Research, Wako, Saitama 351-0198, Japan, the [§]Department of Academic Research Support Promotion Facility, Center for Research Promotion and Support, Fujita Health University, Toyoake, Aichi 470-1192, Japan, the [¶]Collaborative Research Institute for Innovative Microbiology, Department of Biotechnology, Graduate School of Agricultural and Life Sciences, University of Tokyo, Tokyo 113-8657, Japan, and the **Department of Computational Biology and Medical Sciences, Graduate School of Frontier Sciences, University of Tokyo, Kashiwa, Chiba 277-8561, Japan*

Edited by Gerald W. Hart

In eukaryotic cells, unconjugated oligosaccharides that are structurally related to *N*-glycans (*i.e.* free *N*-glycans) are generated either from misfolded *N*-glycoproteins destined for the endoplasmic reticulum–associated degradation or from lipid-linked oligosaccharides, donor substrates for *N*-glycosylation of proteins. The mechanism responsible for the generation of free *N*-glycans is now well-understood, but the issue of whether other types of free glycans are present remains unclear. Here, we report on the accumulation of free, *O*-mannosylated glycans in budding yeast that were cultured in medium containing mannose as the carbon source. A structural analysis of these glycans revealed that their structures are identical to those of *O*-mannosyl glycans that are attached to glycoproteins. Deletion of the *cyc8* gene, which encodes for a general transcription repressor, resulted in the accumulation of excessive amounts of free *O*-glycans, concomitant with a severe growth defect, a reduction in the level of an *O*-mannosylated protein, and compromised cell wall integrity. Our findings provide evidence in support of a regulated pathway for the degradation of *O*-glycoproteins in yeast and offer critical insights into the catabolic mechanisms that control the fate of *O*-glycosylated proteins.

N- and *O*-glycosylations are major forms of co- and post-translational modifications in eukaryotes. The explosive advances in the field of glycobiology during the past 2 decades have revealed not only the pathways for the biosynthesis of glycans but also how glycans function in various biological processes, such as protein quality control, protein targeting, signal transduction, cell–cell interactions, immune responses, cell differentiation, and cancer metastasis (1, 2).

In the ER[3] of budding yeast, *Saccharomyces cerevisiae*, *N*-glycosylation reactions are initiated by transferring an oligosaccharide composed of 14 sugars ($Glc_3Man_9GlcNAc_2$) from lipid-linked oligosaccharides (LLOs) to Asn residues in the consensus sequence, Asn-Xaa-Ser/Thr (where Xaa is any amino acid except Pro), of nascent polypeptide chains (3, 4). The immature *N*-glycoproteins are then assisted by various ER-resident molecular chaperones, such as BiP, calnexin, and peptide disulfide isomerase, to achieve the correct protein folding and/or the formation of protein complexes. In this process, *N*-glycans are recognized as "tags" that dictate the folding status of the carrier proteins (5–8).

Several studies of budding yeast have shown that *O*-mannosylation is involved in these two major biological processes. One is related to cell wall integrity. The rigid and protective layer of the cell wall, composed of heavily *O*-mannosylated and/or *N*-glycosylated proteins, is essential for cell viability and correct cell division during vegetative growth as well as under conditions of environmental stress (*e.g.* heat stress and proteolysis) (9, 10). Mutants that are defective in the key *O*-mannosylation enzyme therefore exhibit slow growth due to the lack of cell wall integrity (11, 12). The other pivotal function of *O*-mannosylation in the biological process is the quality control of newly synthesized proteins in the ER. It has been reported that some *O*-glycosylated model ERAD substrates, including α-factor, Gas1*, and KHNt, undergo excessive *O*-mannosylation by protein *O*-mannosyltransferases 1 and 2 (Pmt1 and Pmt2) (13, 14) and that Pmt1 and Pmt2 interact with the component of the luminal surveillance complex for ERAD, Hrd1, to facilitate the

This work was supported by Japan Science Society Sasakawa Scientific Research Grant 24-411 (to H. H.), the Society of Yeast Scientists (Japan) Dr. Yoshifumi Jigami Memorial Fund (to H. H.), Japan Society for the Promotion of Science (JSPS) Grant-in-Aid for Young Scientists (B) 16K18521 (to H. H.), a research grant from Noda Institute for Scientific Research (NISR) (to H. H.), JSPS Grant-in-Aid for Scientific Research (B) 25291030 (to T. S.), the Mizutani Foundation for Glycoscience (to T. S.), and a RIKEN pioneering project (glycolipidologue initiative) (to T. S.). The authors declare that they have no conflicts of interest with the contents of this article.
This article was selected as one of our Editors' Picks.
RNA-Seq data used in this study were deposited in the NCBI database under accession number GSE130332.

[1] A Japan Society for the Promotion of Science (JSPS) Postdoctoral Fellow (PD).
[2] To whom correspondence should be addressed. Tel.: 81-48-467-9614; Fax: 81-48-462-4692; E-mail: tsuzuki_gm@riken.jp.

[3] The abbreviations used are: ER, endoplasmic reticulum; LLO, lipid-linked oligosaccharide; ERAD, endoplasmic reticulum–associated degradation; FNG, free *N*-glycan; PNGase, peptide:*N*-glycanase; FOG, free *O*-glycan; PKC, protein kinase C; PA, pyridylamination; CFW, calcofluor white; CR, Congo red; OD, optical density; Man'ase, mannosidase.

degradation of excessive *O*-mannosylated misfolded proteins (15). Moreover, in a recent study, Xu *et al.* (16) clearly showed that *O*-mannosylation executed by Pmt1 and Pmt2 terminates attempts of long-retained misfolded proteins to undergo folding in the ER and facilitates their degradation. It therefore appears that both *N*- and *O*-glycosylation are critical for the recognition and elimination of misfolded glycoproteins in the ER (16).

In addition to *N*- and *O*-glycans on proteins in the secretory pathway, it is known that "free," unconjugated forms of oligosaccharides related to *N*-glycans (free *N*-glycans; FNGs) can accumulate in the cytosol in eukaryotic cells (17–26).There are two major pathways for the generation of FNGs in budding yeast (21, 25). First, in the peptide:*N*-glycanase (PNGase)-dependent pathway, FNGs are generated from misfolded glycoproteins by the action of a cytosolic PNGase (Png1). In the second, the oligosaccharyltransferase-dependent pathway, mature forms of dolichol-linked oligosaccharides ($Glc_3Man_9GlcNAc_2$) are liberated in the luminal side of the ER by oligosaccharyltransferase. The FNGs that accumulate in the ER are then processed by glycosidases in the ER and are eventually transported to the cytosol by an unidentified mechanism. The biological relevance of the formation/degradation of FNGs is, however, poorly understood.

During our studies dealing with the functional importance of FNG generation, we analyzed the free oligosaccharides that had accumulated in yeast cells under various culture conditions. Surprisingly, novel forms of free oligosaccharides were observed when the cells were cultured in media containing mannose as the carbon source. Extensive structural analyses clearly indicated that these oligosaccharides are structurally identical to the *O*-mannosyl glycans that are covalently attached to yeast glycoproteins. We hypothesized that the free *O*-glycans (FOGs) are probably liberated from *O*-glycoproteins by a putative endo-*O*-α-mannosidase–like activity. We also showed that the formation of FOGs is regulated by the general transcription repressor Cyc8, and further analyses suggested that the hyperactivation of the FOG generation pathway may result in the dysregulation of protein kinase C (PKC)-mediated cell wall integrity. Our results thus imply that a novel mechanism exists for regulating the catabolism of *O*-mannosyl glycans in yeast.

Results

Generation of the novel free oligosaccharides produced in yeast

The findings reported in our previous studies suggested that the yeast cytosolic/vacuolar α-mannosidase, Ams1, plays a pivotal role in the catabolism of FNGs that accumulate in the cytosol (22, 25, 27). Several studies have shown that the intrinsic expression level and enzymatic activity of Ams1 are significantly increased under certain specific culture conditions, such as cell wall stress, deprivation of the carbon source, and starvation caused by insufficient nitrogen sources (22, 25, 28). To understand the molecular mechanisms for the activation of the Ams1-dependent degradation of FNGs, we cultured yeast cells in various culture media for 3 h at 30 °C and profiled the structure of the PA-labeled FNGs by size-fractionation HPLC analysis. In normal culture media, YPGlc, the major form of FNGs was $Hex_{7-9}HexNAc_2$, as reported previously (22, 29). In contrast, the generation of FNGs was reduced when certain types of culture media, such as YPGal, YPGly, and YP, were used, probably due to the intracellular activation of Ams1. This result is consistent with previous observations that Ams1 activity is increased when the level of glucose in the culture media is reduced (25, 27). On the other hand, we unexpectedly discovered that large amounts of novel free oligosaccharides were produced only when the cells were grown in the YPMan medium (Fig. 1*A*, *peaks a–d*). The oligomers corresponding to these peaks were structurally altered on treatment with jack bean α-mannosidase (Fig. 1*B*), suggesting that they are α-mannosylated glycans. These results suggest that, in budding yeast, the generation of novel α-mannosylated free oligosaccharides can be induced by using YPMan as a medium.

Biosynthesis pathway of the novel structure for free glycans

We next attempted to determine the structure of these novel free oligosaccharides. For this purpose, the compounds corresponding to the collected peaks a–d were subjected to structural and linkage analyses. The findings indicated that the MS values for peaks a–d corresponded to those of PA-Hex_{2-5}. Moreover, analyses of these peaks after digestion with various glycosidases clearly indicated that the structures of the PA-Hex_{3-5} glycans (peaks b–d) were identical to those of the *O*-mannosyl glycans in *S. cerevisiae* (see Tables 1 and 2; see Fig. 1*C* for the structures of *O*-mannosyl glycans). We therefore hypothesized that these free glycans are derived from the *O*-mannosyl glycans on glycoproteins. To validate this hypothesis, the total amounts of free glycans in the two mutants that were defective in the first and second steps of mannose transfer reactions, *pmt1*Δ *pmt2*Δ and *ktr1*Δ *kre2*Δ *ktr3*Δ, respectively (see Fig. 1*C* for the transferase responsible for each mannose residue), were quantified. As shown in Fig. 1 (*C* and *D*), a substantial reduction in the level of Man_{2-5} free glycans was observed in the case of the *ktr1*Δ *kre2*Δ *ktr3*Δ cells. This result clearly suggests that the enzymes responsible for the addition of the second α-mannose of *O*-mannosyl glycans on glycoproteins is also required for the formation of Man_{2-5} free oligosaccharides, now designated as FOGs. There are, however, two possible scenarios for how these FOGs could be formed: 1) they are released from *O*-mannosylated glycoproteins by the action of an endo-*O*-α-mannosidase, or 2) they are formed by the same machinery that is involved in *O*-mannosylation by using free mannose as a donor. To distinguish between these two possibilities, cells defective in the first mannose transfer, *pmt1*Δ *pmt2*Δ, were tested for the formation of FOGs. As shown in Fig. 1 (*C* and *D*), a significant reduction in the generation of Man_{2-5} glycans was observed for the *pmt1*Δ *pmt2*Δ cells, indicating that the formation of *O*-mannosyl glycans is likely a prerequisite for the efficient formation of FOGs. This result therefore favors the first scenario (*i.e.* FOGs are formed from protein-linked *O*-mannosyl glycans by the action of an endo-*O*-α-mannosidase). Because the *O*-linked sugar chains are elongated starting at Man1 and proceed to Man5 in early to late Golgi, we suspected that the de-*O*-mannosylation of glycoproteins

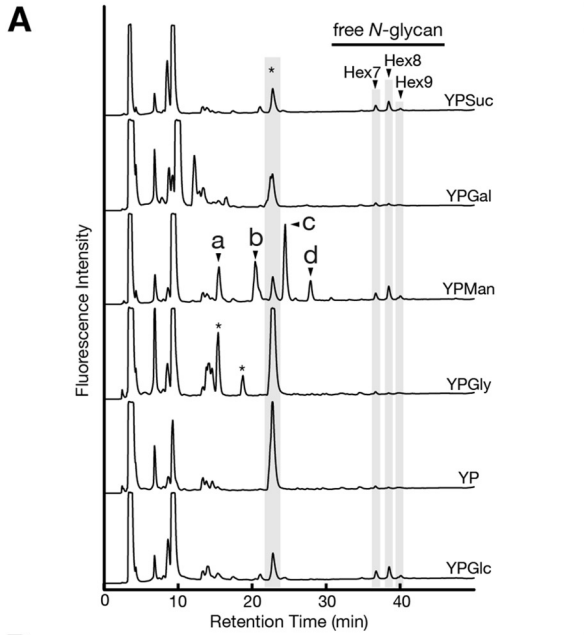
A
free N-glycan
Hex7
Hex8
Hex9
YPSuc
YPGal
YPMan
YPGly
YP
YPGlc
a
b
c
d
Fluorescence Intensity
Retention Time (min)

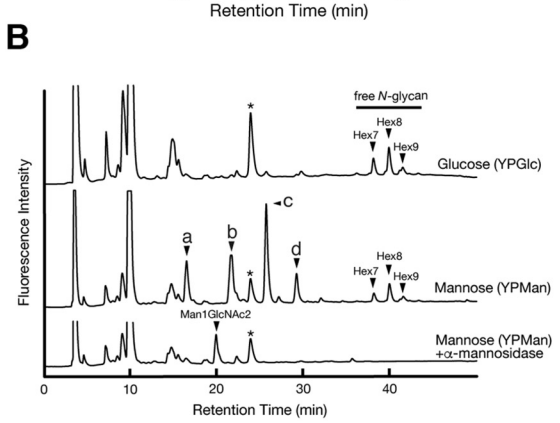
B
free N-glycan
Hex7
Hex8
Hex9
Glucose (YPGlc)
Mannose (YPMan)
Man1GlcNAc2
Mannose (YPMan)
+α-mannosidase
a
b
c
d
Fluorescence Intensity
Retention Time (min)

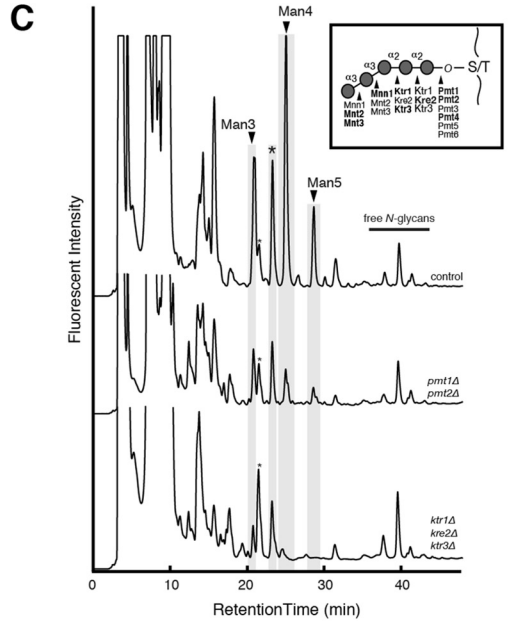
C
Man4
Man3
Man5
free N-glycans
control
pmt1Δ
pmt2Δ
ktr1Δ
kre2Δ
ktr3Δ
Mnn1
Mnt1
Mnt2
Mnt3
Ktr1
Kre2
Ktr3
Pmt1
Pmt2
Pmt3
Pmt4
Pmt5
Pmt6
S/T
Fluorescent Intensity
RetentionTime (min)

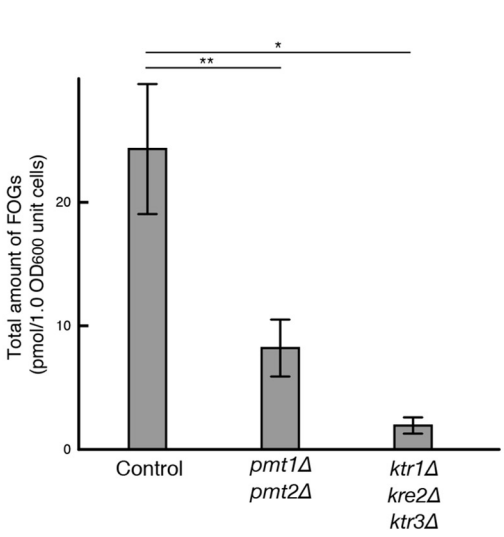
D
Total amount of FOGs
(pmol/1.0 OD600 unit cells)
Control
pmt1Δ
pmt2Δ
ktr1Δ
kre2Δ
ktr3Δ

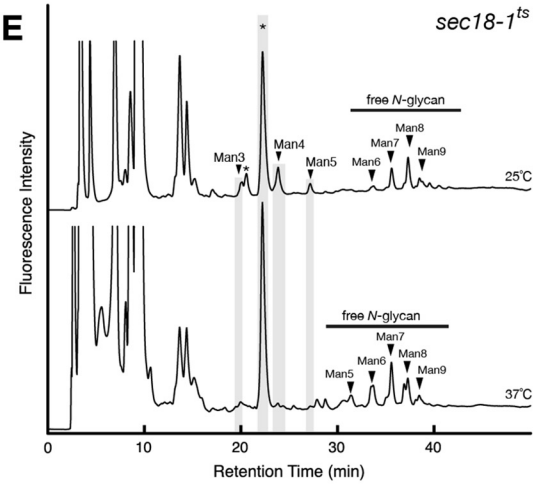
E
sec18-1ts
free N-glycan
Man3
Man4
Man5
Man6
Man7
Man8
Man9
25℃
37℃
Fluorescence Intensity
Retention Time (min)

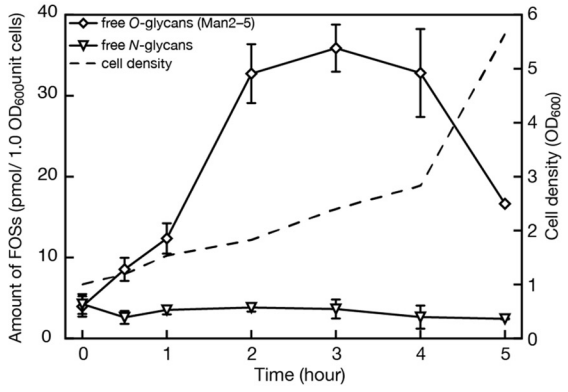
F
free O-glycans (Man2–5)
free N-glycans
cell density
Amount of FOSs (pmol/ 1.0 OD600unit cells)
Cell density (OD600)
Time (hour)

Table 1
MALDI-TOF MS analysis of size-fractionated glycans

Peak	Observed mass (*m*/*z*)	Composition
a	443.0 $[M + Na]^+$	Hex_2-PA
b	605.3 $[M + Na]^+$	Hex_3-PA
c	767.3 $[M + Na]^+$	Hex_4-PA
d	929.5 $[M + Na]^+$	Hex_5-PA

Table 2
Linkage analysis of unidentified glycans

Peak	α-Man' ase	α-1,2-Man' ase	α-1,2/3-Man' ase α-1,2-Man' ase	Predicted structure
a	+	–‡	+	Man_2
b	+	+*	+	Man_3
c	+	–	+	Man_4
d	+	–	+	Man_5

‡ *A. saitoi* α-1,2-Man'ase cannot digest PA-labeled α-1,2-mannobiose, which has a ring-opening mannose moiety in its reducing end.
* Man_3 was converted to Man_2 due to the substrate specificity of *A. saioi* α-1,2-Man'ase as mentioned above.

occurs in a late stage of the secretory pathway. To verify this hypothesis, we examined the generation of FOGs in a *sec18-1* mutant, which is deficient in ER-to-Golgi trafficking at a nonpermissive temperature (37 °C). At the permissive temperature, significant amounts of Man_{2-5} FOGs were generated in *sec18-1* cells. On the other hand, negligible generation of the Man_{2-5} of FOGs was observed at the nonpermissive temperature (37 °C) (Fig. 1*E*), suggesting that functional ER-to-Golgi trafficking is required for the efficient production of FOGs. We also examined the time course for the generation of FNGs and FOGs. The rate of generation of FNGs was essentially unaltered during the time course analysis after changing the medium from YPGlc to YPMan, whereas the total amount of the FOGs in the cells reached a maximum at around 3 h (Fig. 1*F*). These results suggest that the concentration of mannose is a key trigger for the specific activation of the FOG generation pathway.

FOGs were accumulated in the post-Golgi compartment

Whereas it has been clarified that most of the FNGs in the WT are released from misfolded glycoproteins that are destined for ERAD by the action of Png1 (a cytosolic peptide:*N*-glycanase) (21, 25), the subcellular site for the generation of FOGs remains unknown. To clarify this issue, we utilized a reporter protein, Prc1pp-ManLe-FLAG. This reporter protein was composed of three functional domains: 1) the catalytic domain of an α-mannosidase derived from tomato (ManLe), which was successfully expressed by yeast cells as an active, secreted enzyme (30); 2) ER-targeting signal (Prc1-pre); and 3) vacuole-targeting signals (Prc1-pro) (Fig. 2*A*). The second and third domains were derived from a vacuolar protease, Prc1, and these domains were expected to allow this protein to be delivered to the vacuole via the Golgi-to-vacuole sorting receptor, Vps10. The Prc1pp-ManLe-FLAG expressed in *ams1*Δ or *vps10*Δ *ams1*Δ was *N*-glycosylated, indicating that this reporter protein is at least correctly targeted to the ER (Fig. 2*B*). We then proceeded to verify the intracellular amount of FOGs with or without the expression of Prc1pp-ManLe-FLAG. As shown in Fig. 2*C*, the expression of Prc1pp-ManLe-FLAG caused a significant reduction in the levels of FOGs in *ams1*Δ cells. On the other hand, in *vps10*Δ *ams1*Δ cells, the total amount of FOGs in the cell was comparable with that for *ams1*Δ cells with a vector control, possibly due to the defective transport of Prc1pp-ManLe-FLAG and/or its potential substrates to post-Golgi compartments. This result thus indicates that FOGs are, in sharp contrast to the case for most FNGs, generated in the lumenal side of the vesicles and most likely accumulated in a post-Golgi compartment, such as vacuoles.

Intracellular pools of nucleotide sugars and N- and O-glycosylation in YPMan culture conditions

Having confirmed the source of the FOGs, we next examined the issue of how the YPMan culture conditions affect the *N*- and *O*-glycosylation status in yeast. To this end, the levels of nucleotide sugars, as well as the extent of *N*- and *O*-glycosylation on glycoproteins, were quantitated. The biosynthesis of nucleotide sugars is a crucial step for the synthesis of donor substrates for *N*-glycosylation and *O*-mannosylation, dolichol-linked oligosaccharide, and dolichyl-phosphate-mannose (*Dol-P-Man*) (Fig. 3*A*) (4). As shown in Fig. 3*B*, a significant increase of the level of GDP-Man was observed when YPMan was used as the culture medium. In contrast, no increase in the levels of other nucleotide sugars, which are important for the biosynthesis of *N*-glycans, was observed (*i.e.* UDP-Glc and UDP-GlcNAc) (Fig. 3*B*). In addition, despite the increase in GDP-Man levels, the total level of *N*- and *O*-glycans on glycoproteins was comparable between the YPGlc and YPMan culture media (Fig. 3*C*). From these data, we conclude that, in the case of YPMan medium, the levels of both GDP-Man and FOGs were increased, whereas no significant increase in the levels of FNGs, *N*-glycosylation, or *O*-glycosylation was observed. It can therefore be safely assumed that the increase in FOGs is not simply due to the overloaded synthesis of *O*-glycans, but rather a regulated event that is controlled by medium conditions, including the enhanced catabolism of *O*-glycans.

Figure 1. Unknown source of the free oligosaccharides that are generated in cells cultured in mannose-containing medium. *A*, HPLC profile of the free oligosaccharides derived from the yeast cells cultured with various carbon sources (YPSuc, YPGal, YPMan, YPGly, and YPGlc contain 2% sucrose, galactose, mannose, glycerol, and glucose, respectively). YP medium contains no carbon source. *Asterisks* and *Hex7–9* represent nonspecific peaks and those of PA-labeled $Hex_{7-9}HexNAc_2$, respectively. *B*, unknown peaks are sensitive to a jack bean α-mannosidase treatment. *C*, HPLC profile of the FOGs in *pmt1*Δ *pmt2*Δ and *ktr1*Δ *kre2*Δ *ktr3*Δ mutants and the structures of the *O*-glycan in yeast. First, a mannose on Ser/Thr residues on glycoproteins is transferred via the action of the protein *O*-mannose transferase, Pmt1–6. The Golgi-resident α-1,2-mannosyltransferases Ktr1, Kre2, and Ktr3 are involved in the transfer of the second and third mannose units. Two outer mannoses are transferred via the action of α-1,3-mannosyltranferases, Mnn1, Mnt2, and Mnt3. Mannosyltransferases with *boldface letters* are primary enzymes in each transfer step (11, 12). Mutants used this analysis, *pmt1*Δ *pmt2*Δ and *ktr1*Δ *kre2*Δ *ktr3*Δ, are all in *ams1*Δ background. *D*, quantitative analysis of the generation of FOGs of *C*. *E*, HPLC profile of the FOGs/FNGs in *sec18-1* mutant defective in the ER-to-Golgi trafficking. *F*, time course for the generation of FOGs in the cells cultured with YPMan. *Error bars*, S.D. from three independent experiments. For statistical analysis, Student's *t* test was applied. * and **, $p < 0.05$ and $p < 0.01$, respectively.

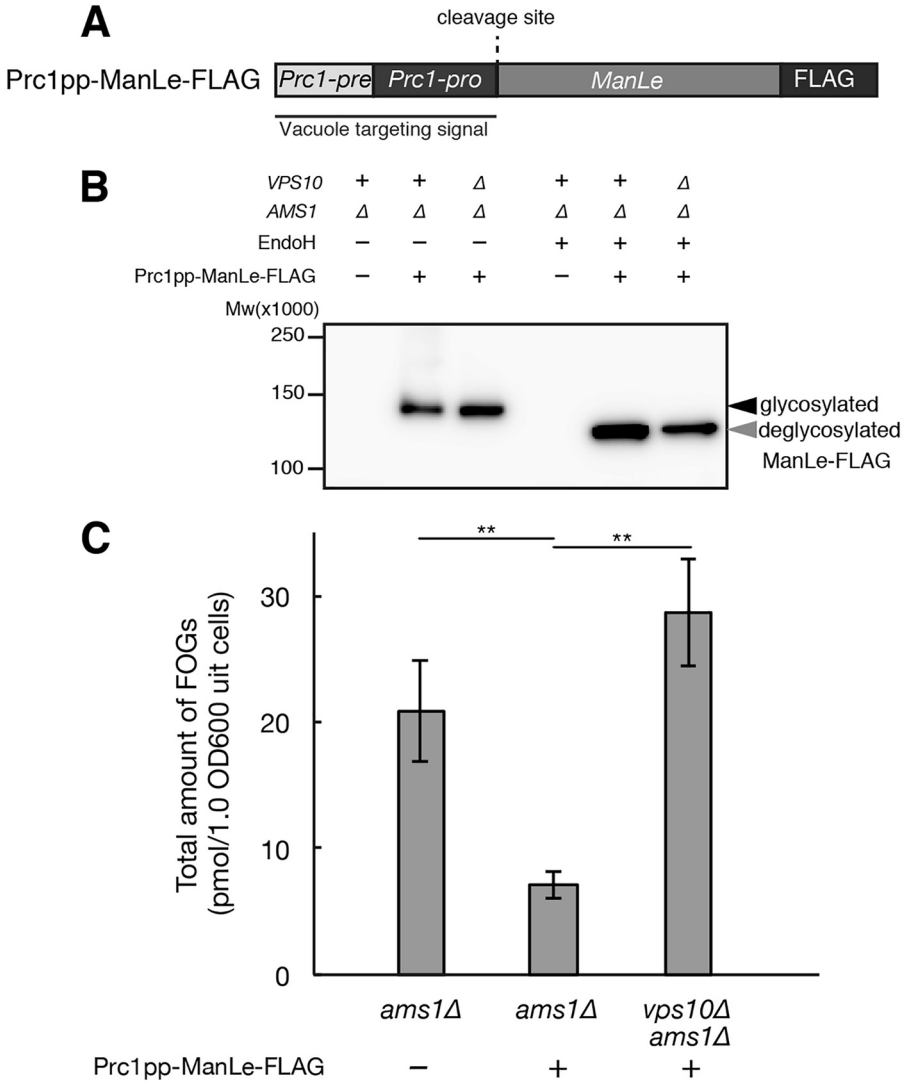

Figure 2. FOGs accumulate in the compartment where the proteins are sorted by Vps10. *A*, *schematic representation* of the primary structure of the ManLe-FLAG fused with the vacuole-targeting signals of Prc1, the Prc1-pre/pro sequence. *B*, expression level and glycosylation status of ManLe-FLAG in *ams1*Δ and *vps10*Δ *ams1*Δ are analyzed by immunoblot analysis. *C*, accumulated FOGs are sensitive to the Prc1pp-ManLe-FLAG that is targeted to the late secretory pathway in Vps10-dependent fashion. *Error bars*, S.D. from three independent experiments. For statistical analysis, Student's *t* test was applied. **, $p < 0.01$.

The generation of FOGs is negatively regulated by the general transcription repressor, Cyc8

To gain additional insights into the regulation of the formation of FOGs under YPMan culture conditions, we examined the effect of glucose concentration in the culture media. As shown in Fig. 4*A*, small but significant amounts of FOGs were generated when a medium containing 1% glucose and 1% mannose was used. Most importantly, when a medium containing 0.2% glucose and 2% mannose was used, the generation of FOGs was significantly inhibited compared with a medium containing only 2% mannose (compare the *first* and *second column* of Fig. 4*A*). This fact led us to assume that the generation of FOGs is not only induced by the presence of mannose but is also strictly repressed by the presence of glucose in the media. We therefore further investigated the issue of whether the transcription factors involved in the regulation of catabolite repression also regulate the generation of FOGs. As shown in Fig. 4*B*, a deletion strain of one component of the general transcription repressor complex for glucose repression (*i.e. cyc8*Δ cells) exhibited a drastic increase (~10-fold) in the generation of the FOGs. However, the deletion of other components of the repressor complex (*i.e. mig1*Δ and *tup1*Δ) showed no dramatic increase in the generation of FOGs, suggesting that Cyc8 is specifically involved in regulating the generation of FOGs.

During the analysis of the FOGs in *cyc8*Δ cells, we also found that *cyc8*Δ grew more slowly than usual in YPMan medium. To dissect this phenotype further, *cyc8*Δ cells were cultured on plates containing several different carbon sources. As shown in Fig. 4*C*, attempts to grow *cyc8*Δ cells on YPMan plates resulted in severely retarded growth, whereas this was not observed for YPGlc or YPSuc plates, suggesting that the growth defect phenotype of *cyc8*Δ is specific for YPMan media. We further examined the detailed phenotype of the growth defect of *cyc8*Δ under various conditions (*e.g.* high temperature and the addition of cell wall perturbation reagents, calcofluor white (CFW) or Congo red (CR)). When cultured under YPMan at 30 and 36 °C, the *cyc8*Δ cells exhibited a strong growth defect (Fig. 4*D*, *second* and *third panels*). Furthermore, the *cyc8*Δ cells showed a strong

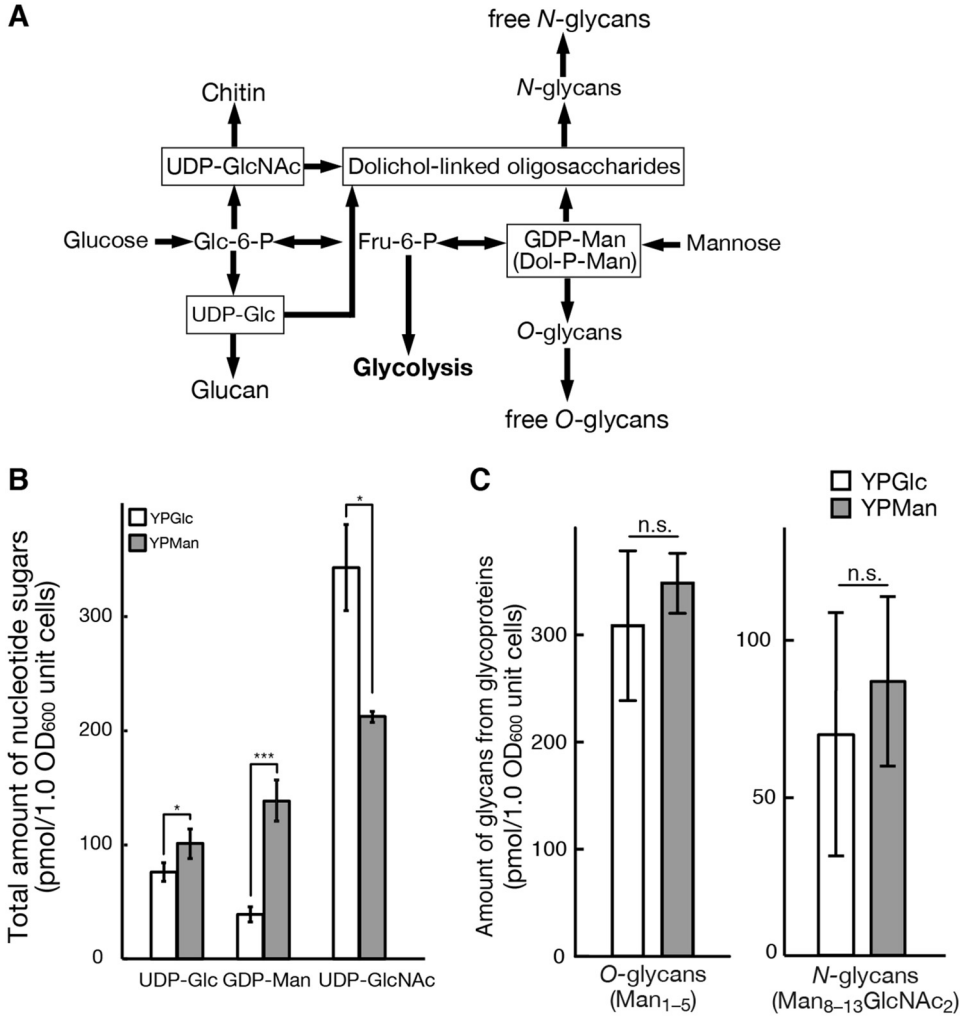

Figure 3. Quantitative analysis of the total amount of nucleotide sugars and *N*- and *O*-glycans on glycoproteins. After cultivating the cells in YPGlc or YPMan for 3 h, the levels of nucleotide sugars and *N*- and *O*-glycans on glycoproteins were determined. *A*, *schematic representation* of the biosynthetic pathway for nucleotide sugars, cell wall polymers, and glycans. For statistical analysis, a Tukey–Kramer test was used to calculate the difference between the groups. *B*, total amount of GDP-Man is significantly increased in the case of cells cultured in YPMan. For statistical analysis, Student's *t* test was used to calculate differences between groups. *C*, the generation of *N*- and *O*-glycans on glycoproteins is comparable in both of the culture conditions (*i.e.* YPGlc and YPMan). *Error bars*, S.D. from three independent experiments. *n.s.*, *, **, and ***, not significant, $p < 0.05$, $p < 0.01$, and $p < 0.005$, respectively.

sensitivity to YPMan supplemented with CFW or CR (Fig. 4*D*, *fourth* and *fifth panels*) even at 25 °C, indicating that the integrity of the cell walls in these cells had been compromised. Notably, these growth defect phenotypes were mitigated in YPGlc media, leading us to hypothesize that the hyperactivation of FOG formation and the loss of cell wall integrity could be a related event, possibly through the excessive de-*O*-mannosylation of cell wall proteins and/or secretory proteins.

Hyperactivation of the generation of FOGs disrupts the cell wall integrity pathway (PKC signaling pathway)

Based on the fact that *cyc8*Δ cells show a cell wall defect phenotype in YPMan media, we suspected that the cell wall integrity pathway (PKC pathway) in these cells had been compromised. To validate this hypothesis, the phosphorylation status of Mpk1, an intermediate in the PKC pathway, was examined using a phosphorylated Mpk1-specific antibody (Fig. 5*A*). As shown in Fig. 5*B*, Mpk1 was phosphorylated only when cells were exposed to the cell wall stressor reagent, CFW, in WT cells. In contrast, when *cyc8*Δ cells were cultured in YPMan medium, Mpk1 was found to be constitutively phosphorylated. Moreover, no further increase in the levels of phosphorylated Mpk1 was observed in these cells upon CFW treatment in YPMan medium. Those results clearly suggest that PKC signaling is dysregulated in *cyc8*Δ cells by YPMan media. We further examined *O*-mannosylation status as well as the expression level of the cell wall sensor protein, Wsc1, which is known to be a heavily *O*-mannosylated protein through a serine/threonine cluster in their stem region that is located in the extracellular space (31). As expected, a substantial reduction in the total amount of Wsc1 was observed in the *cyc8*Δ cells cultured with YPMan (Fig. 5*C*). It should be noted that, by the RNA-Seq analysis for profiling gene expression patterns among the different carbon sources, we did not find significant changes in the transcription level of *WSC1* in WT and *cyc8*Δ in the YPMan culture for 180 min, as compared with culturing these cells with YPGlc for 180 min (Fig. 5, *D* and *E*), suggesting that the reduction of the expression level of Wsc1 in *cyc8*Δ cells cultured with

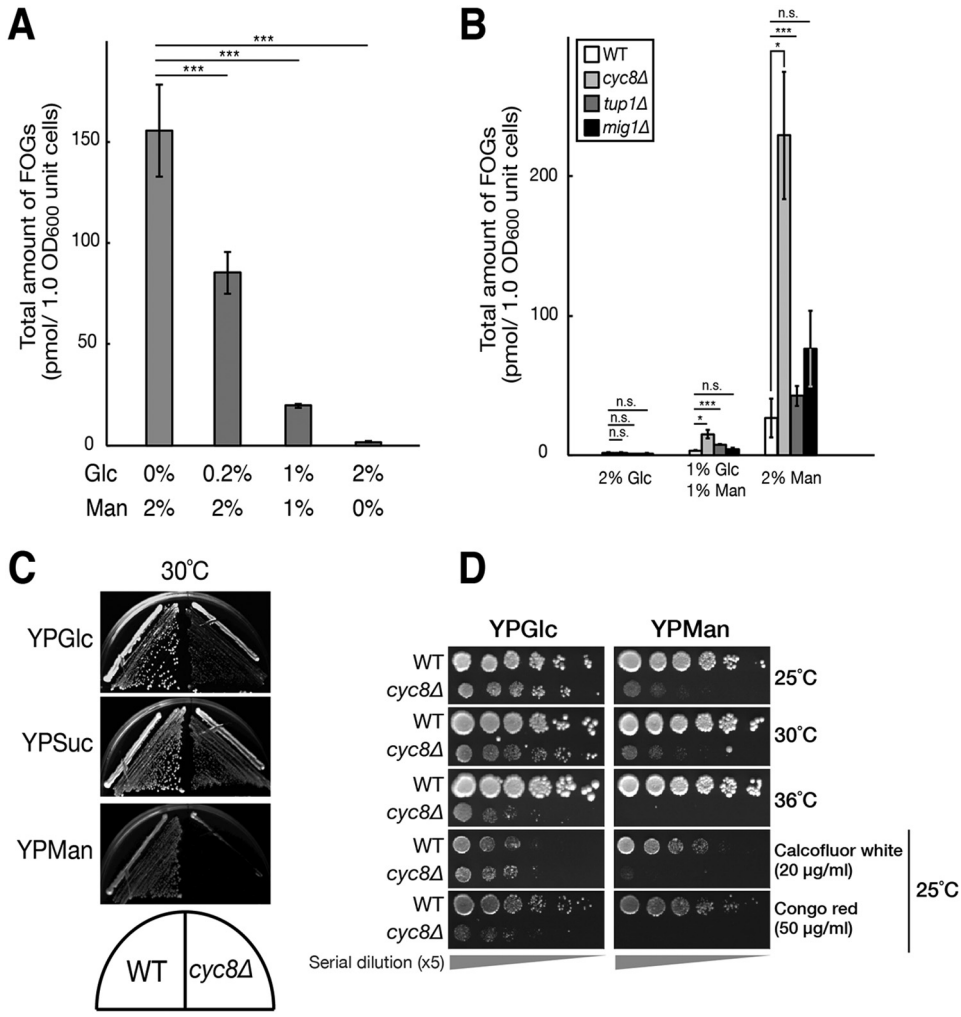

Figure 4. Generation of FOGs is strictly controlled by the general transcriptional co-repressor, Cyc8. *A*, generation of FOGs is suppressed by the addition of glucose in the YPMan medium. *B*, disruption of *CYC8* gene causes hyperactivation of the FOG generation pathway. *C*, growth phenotype of *cyc8*Δ cells on the plates containing several carbon sources. *D*, spotting assay of *cyc8*Δ cells. Serial diluted cells (×5) were spotted on the plates. *Error bars*, S.D. from three independent experiments. For statistical analysis, Student's *t* test was applied. *n.s.*, *, **, and ***, not significant, $p < 0.05$, $p < 0.01$, and $p < 0.005$, respectively.

YPMan is not due to the transcriptional suppression of *WSC1* but rather the post-transcriptional regulation of Wsc1 proteins. Collectively, these results indicate that in budding yeast, the Wsc1 protein in *cyc8*Δ cells cultured with YPMan might cause an instability and dysfunction in the Wsc1 protein. It could therefore be assumed that the demannosylation of Wsc1-HA, presumed to be up-regulated in *cyc8*Δ cells cultured with YP Man media, may be involved in the destabilization of the Wsc1-HA protein, which could be a mechanistic basis for the dysregulation of the PKC pathway in *cyc8*Δ cells.

Discussion

The generation and catabolism of free oligosaccharides derived from glycoproteins as well as LLOs are fundamental phenomena that occur from bacteria to mammalian cells (17, 18, 32). However, most studies have focused on the generation of FNGs (*i.e.* free oligosaccharides that are structurally related to *N*-glycans). Although Iwatsuka *et al.* (33) reported the detection of extracellular FOGs with structures similar to mucin-type *O*-glycan chains in human sera, the occurrence of intracellular FOGs has not been reported in any system. In this study, we serendipitously discovered that a series of novel free glycans that are structurally related to *O*-mannosyl glycans are produced only when the yeast cells are cultured in media containing mannose as the sole carbon source. Structural analyses of the FOGs showed that they are structurally identical to *O*-mannosyl glycans that are attached to yeast glycoproteins. Consistent with this assumption, PA-Man_{2-5} prepared from yeast *O*-mannosyl glycans was found to co-migrate with the PA-Man_{2-5} peaks of FOGs when compared by dual-gradient reversed-phase HPLC (34).[4] We conclude that these FOGs are generated by the action of a putative endo-*O*-α-mannosidase to *O*-mannosyl glycoproteins because 1) the *pmt1*Δ *pmt2*Δ mutant, which is defective in the first mannose transfer to Ser/Thr residues in acceptor proteins, also showed a significantly reduced generation of FOGs (Fig. 1*D*), indicating that *O*-mannosylation is prerequisite for the formation of FOGs, and 2) the addition of pNP-α-Man to the YPMan media did not result in the lengthening of the oligomannose structures on this com-

[4] H. Hirayama, T. Matsuda, Y. Tsuchiya, R. Oka, J. Seino, C. Huang, K. Nakajima, Y. Noda, Y. Shichino, S. Iwasaki, and T. Suzuki, unpublished data.

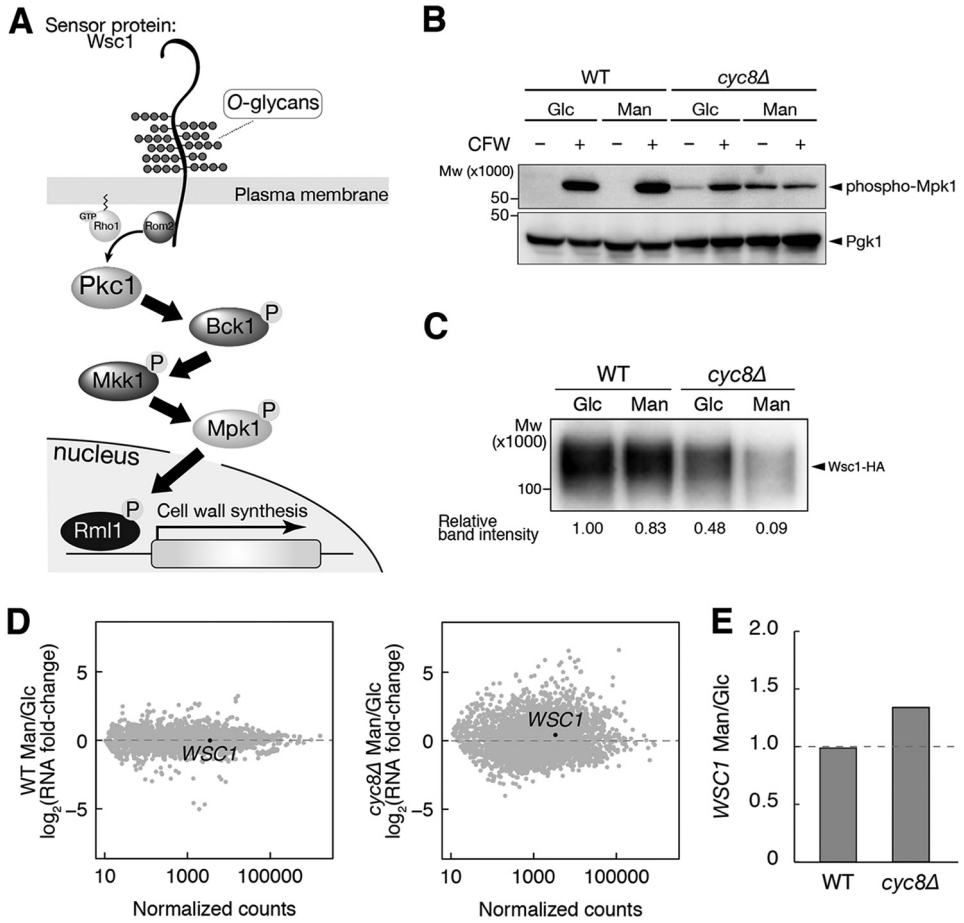

Figure 5. Aberrant processing of *O*-glycosylation in the cell surface sensor protein for the cell wall integrity pathway, Wsc1, may cause the constitutive activation of Mpk1 in *cyc8*Δ cells. *A*, *schematic representation* of the cell wall integrity signaling pathway. *B*, immunoblot analysis of phosphorylated Mpk1 by an anti-phosphorylated Mpk1 antibody with or without activation of the cell wall integrity pathway by 20 μg/ml CFW in YPGlc of YPMan media. *C*, immunoblot analysis of Wsc1-HA in WT and *cyc8*Δ cell culture with YPGlc or YPMan. The relative amount of Wsc1-HA is indicated at the *bottom* of each *lane*. *D*, analysis of transcriptional regulation of Wsc1 under YP Man culture. MA plot for differential expression analysis in WT and *cyc8*Δ cells. The mean of read counts normalized to library size *versus* the $\log_2$ -fold change between YPMan and YPGlc media was shown. The *WSC1* gene is highlighted as a *black dot*. *E*, relative transcription level of *WSC1* in WT and *cyc8*Δ cells shown in Fig. 5*D*.

pound,[5] implying that elongation of *O*-mannosyl glycans likely occurs on the glycoprotein itself. At present, however, the possibility of the direct lengthening of oligomannose structures with free mannose as an acceptor cannot be completely excluded. Irrespective of their sources, when we induce ER stress in yeast, FOGs were not observed, indicating that mere ER stress is not sufficient to induce the formation of FOGs (25).

It has been reported that, in yeast, FNGs accumulate in the cytosol and are processed by α-mannosidases, Ams1, that are localized in cytosol/vacuoles (25, 26, 27). In contrast, FOGs were predicted to be localized in the lumenal side of vesicles, because they are susceptible to digestion by the lumenal α-mannosidase, Prc1pp-ManLe-FLAG. Because the digestion reaction was found to be Vps10-dependent, it was assumed that either substrates (*O*-mannosylated proteins) or the ManLe enzyme needed to be delivered to post-Golgi compartments, such as vacuoles, thus facilitating the demannosylation reaction (Fig. 2). This result is further supported by the observation that the overexpression of Ams1 in *atg19*Δ cells, which causes Ams1 to be exclusively localized in the cytosol, did not result in a reduction of the levels of FOGs, whereas a significant reduction in FNGs was observed.[5] However, the precise location where FOGs are generated currently remains unclear. Efforts are currently under way to identify factors, including a putative de-*O*-mannosylation enzyme (endo-*O*-α-mannosidase), that might be involved in the generation of FOGs to clarify this issue.

GDP-Man levels were increased when YPMan medium was used, suggesting that the intracellular pool of mannose is the rate-limiting step in the synthesis of GDP-Man (Fig. 3*B*). On the other hand, despite the fact that substantial amounts of FOGs were generated when YPMan medium was used, the total amounts of *N*- and *O*-glycans on glycoproteins were not significantly altered (Fig. 3*C*). It should also be noted that the total amount of FOGs observed after a 3-h culture with YPMan was about one-tenth that of the *O*-glycans on glycoproteins (compare Figs. 1*E* and 3*C*), indicating that formation of FOGs is likely to be a regulated event and that only a subset of the *O*-mannosyl glycans are released, even under specific conditions such as in YPMan media. Collectively, the increase in the total amount of intracellular FOGs was associated not only with the overloaded synthesis of the donor substrate, GDP-Man, but

[5] H. Hirayama, T. Matsuda, Y. Tsuchiya, R. Oka, J. Seino, C. Huang, K. Nakajima, Y. Noda, Y. Shichino, S. Iwasaki, and T. Suzuki, unpublished observation.

Table 3
Yeast strains used in this study

Strain name	Plasmid	Genotype	Source
BY4741		*MAT***a** *his3Δ1 leu2Δ0 met15Δ0 ura3Δ0*	Laboratory strain
W303-1A		*MAT***a** *leu2-3,112 his3-11 ade2-1 ura3-1 trp1-1 can1-100*	Laboratory strain
YS63-1C		*MAT***a** *sec18-1 leu2 ura3 trp1 his3*	Laboratory strain
YME2093		*MAT***a** *ams1Δ::hphNT1 pmt1Δ::kanMX4 pmt2Δ::His3MX6* BY4741	This study
YME2090		*MAT***a** *ams1Δ::His3MX6 ktr1Δ::hisG kre2Δ::hisG ktr3Δ::hisG* W303	This study
*cyc8*Δ		*MAT***a** *cyc8Δ::kanMX4* BY4741	Open Biosystems
*tup1*Δ		*MAT***a** *tup1Δ::kanMX4* BY4741	Open Biosystems
*mig1*Δ		*MAT***a** *mig1Δ::kanMX4* BY4741	Open Biosystems
YHH027	pRS416-WSC1-HA	*MAT***a** BY4741	This study
YHH031	pRS416-WSC1-HA	*MAT***a** *cyc8Δ::kanMX4* BY4741	This study
YHH120	pRS416GPD-Prc1pp-ManLe	*MAT***a** *ams1Δ::kanMX6* BY4741	This study
YHH121	pRS416GPD-Prc1pp-ManLe	*MAT***a** *ams1Δ::His3MX6 vps10Δ::kanMX4* BY4741	This study
YHH130	pRS316	*MAT***a** *ams1Δ::kanMX6* BY4741	This study

also with the enhanced release of *O*-mannosylated glycans from proteins, both of which would be regulated by medium conditions.

It was also found that, in *cyc8*Δ cells, a marked increase (~10 times) in the generation of FOGs was observed when cultured in YPMan medium, suggesting that the generation of FOGs is strictly regulated by Cyc8 (Fig. 4*B*). However, no FOGs were observed to be produced in *cyc8*Δ cells when they were cultured in YPGlc medium (Fig. 4*B*), strongly indicating that at least two factors are essential for the generation of FOGs in yeast: 1) transcriptional derepression of the genes (by removing glucose from the media) involved in the generation of FOGs and 2) sensing of the presence of mannose in the media. It is noteworthy that the deletion of other binding partners of Cyc8 (*i.e.* Mig1 and Tup1, which are also involved in the transcriptional repression by glucose) did not result in a significant increase in the generation of FOGs (Fig. 4*B*). Further study will be required for an understanding of the detailed mechanism by which Cyc8 controls the generation of FOGs. One potential explanation is that unidentified binding partners for Cyc8 could be involved in regulating the generation of FOGs. This hypothesis is consistent with the fact that each deletion mutant of any of the 12 known binding partners for Cyc8 (Mig1, Crt1, Rox2, Nrg1, Sko1, Cup9, Sut1, Aft1, Cin5, Skn7, Pdh1, and Yap6) (35) still did not result in any significant increase of the generation of FOGs.[5] An alternative (but distant) possibility is that the intrinsic prion-like aggregation property of Cyc8, which is caused by an internal Q-rich sequence (36), might somehow regulate the formation of FOGs that are produced in YPMan media.

In addition to the excessive generation of FOGs, *cyc8*Δ cells also exhibited some severe growth defects in YPMan, consistent with a cell wall defect, implying that the hyperactivation of the de-*O*-mannosylation pathway may affect the integrity of the cell wall. To the best of our knowledge, this is the first report of a yeast mutant showing a sensitivity against YPMan media. It was also clearly shown that the PKC pathway in *cyc8*Δ cells was dysregulated, accompanied by constitutive activation and no further up-regulation upon CFW treatment in YPMan media (Fig. 5*B*). These data lead us to propose that the dysfunction of Wsc1 may accelerate the development of severe cell wall defects and cell death, and it is also tempting to speculate that the excessive de-*O*-mannosylation may be involved in the malfunction of Wsc1. In this connection, it should be noted that mutants defective in *O*-mannosylation were also unstable in Wsc1 and, accordingly, would fail to inactivate the PKC pathway (37).

In summary, in this study, we report on the production of novel types of free oligosaccharides, when yeast cells are cultured in YPMan medium. We identified the structures of those glycans and found that they are structurally identical to those of O-mannosyl glycans. FOGs are most likely formed by the de-*O*-mannosylation of glycoproteins, and the reaction appears to be regulated by the Cyc8 transcriptional repressor. *cyc8*Δ cells exhibited a sensitivity toward YPMan media, with a compromised cell wall integrity, implying the existence of a link between those phenotypic consequences and FOG formation. Clarification of the detailed mechanism responsible for FOG formation will provide answers regarding the biological and physiological relevance of the generation/catabolism of FOGs.

Experimental procedures

Yeast strains and culture conditions

The yeast strains used in this study are summarized in Table 3. Disruption of genes was performed by one-step PCR methods (38). Yeast cells were transformed by the LiOAc method (39). Yeast cells were grown in YPGlc (2% peptone, 1% yeast extract, and 2% glucose) medium. For the generation of FOGs, yeast cells were grown in YPMan (2% peptone, 1% yeast extract, and 2% mannose) medium for 3 h. For the culture of cells harboring plasmids, CASC medium (0.67% yeast nitrogen base without amino acid, 0.5% casamino acid, and 2% glucose) were used. Incubations were carried out at 30 °C unless noted otherwise.

Plasmids used in this study

pRS416-WSC1-HA was a generous gift from Dr. Sabine Strahl (Heidelberg University) (37). For the construction of pRS416GAP-Prc1pp-ManLe-FLAG, the cDNA sequence coding tomato (*Lycopersicon esculentum*) acidic α-mannosidase, ManLe (GenBank™ accession number AC209509.1) (30) was chemically synthesized and cloned into pTAC2 by Fasmac (Kanagawa, Japan) as a PCR template. The following pair of DNA fragments was then amplified: 1) 3012 bp of ManLe fused with FLAG by PCR from pTAC2-ManLe using the following pair of primers, pRS416GPD-pp-SmaI-ML1-F (5′-AACAAGGGATCCCCCGGGAAATATATGGTCTACAACACTT-3′) and pRS416GPD-pp-EcoRI-ML1-FLAG-R (5′-GCTTGATATCGAATTCTCATTTATCATCATCATCTTTATAATCT-

AAGGACATGTGAGATTTC-3′); 2) 336 bp of Prc1-pre/pro signal sequence by PCR from genomic DNA of the BY4741 strain using the following pair of primers, pRS4x6-SpeI-Prc1pp-F (5′-CAAATCTAGAACTAGTATGAAAGCATTC-ACCAGTTTA-3′) and pRS4x6-SpeI-Prc1pp-R (5′-GCAGCC-CGGGGGATCCCTTGTTGACACGAAGCTGA-3′). Those two DNA fragments were fused by overlap-extension PCR using pRS4x6-SpeI-Prc1pp-F and pRS416GPD-pp-EcoRI-ML1-FLAG-R primers. The Prc1pp-ManLe-FLAG fragment was then cloned into pRS416GPD digested with SpeI and EcoRI using an In-Fusion HD cloning kit (TaKaRa, Kyoto, Japan) according to the manufacturer's protocol.

Preparation of pyridylaminated FOGs

Free oligosaccharides including FOGs were prepared as described previously with minor modifications (25). After growing the cells overnight, 10 OD_{600} units of cells were re-inoculated into 10 ml of YPMan media and incubated for 3 h at 30 °C to induce the generation of FOGs. The cells were then collected and washed with PBS. For the disruption of the cells, the collected cells were resuspended in 1 ml of 70% ethanol and centrifuged at 20,000 × *g* for 5 min at 4 °C. The resultant supernatant was collected and evaporated to dryness in a SpeedVac concentrator. For desalting the sample, the dried samples were dissolved in water and applied to a column of ion-exchange chromatography resin (*i.e.* AG1-X2 (resin volume, 500 μl; 200–400 mesh; acetate form)) followed by a column of AG50-X8 (resin volume, 500 μl; 200–400 mesh; H^+ form) (Bio-Rad), and the flow-through fractions containing neutral free oligosaccharides were evaporated to dryness. Pyridylamination of the isolated FOGs was performed as described previously (25).

Preparation of pyridylaminated N- and O-glycans derived from glycoproteins

For the isolation of *N*- and *O*-glycans from glycoproteins, whole glycoproteins were extracted by a hot citrate extraction method as described previously (40). *N*-Glycans and *O*-glycans were released by a PNGase F treatment and hydrazinolysis, respectively, as described previously (40, 41). The desalting and PA-labeling of the glycans were performed as described under "Preparation of pyridylaminated FOGs."

Digestion of free glycans with a glycosidase

Digestion of the FOGs by glycosidases was carried out as described previously (25). Briefly, for the digestion of FOGs with jack bean α-mannosidase (40 milliunits; Seikagaku Corp., Tokyo, Japan) or *Aspergillus saitoi* α-1,2 mannosidase (0.5 milliunits; Seikagaku Corp.), the samples, in 20 μl of the 50 mM of sodium acetate buffer (pH 5.0) at 37 °C, were incubated with the enzymes for 6 h. The digestion of FOGs with *Xanthomonas manihotis* α-1,2/3-mannosidase (60 units; New England Biolabs, Beverly, MA) was carried out in a 20 μl of reaction buffer supplied by the manufacturer at 37 °C for 6 h. The enzyme reaction was terminated by adding 100 μl of 100% ethanol to the incubation. After centrifuging the samples at 20,000 × *g* for 5 min at 4 °C to remove insoluble materials, the supernatant was evaporated to dryness, and the residue was then resuspended in water for HPLC analysis.

HPLC analysis of glycans

Size fractionation HPLC with a Shodex NH2P-40 3E column (3.0-mm inner diameter × 250 mm, Shodex, Tokyo, Japan) was performed as described previously (27). The elution involved the use of two solvent gradients, solvent A (93% acetonitrile in 0.3% acetate (pH 7.0)) and solvent B (20% acetonitrile in 0.3% acetate (pH 7.0)). The column temperature was set at 25 °C, and the flow rate was 0.45 ml/min. The gradient program was as follows: 0–0.5 min, 1–10% solvent B; 0.5–45 min, 10–55% solvent B; 45.1–47 min, isocratic 70% solvent B; 47.1–67.1 min, isocratic 1% solvent B. For the quantification of the peak areas, each peak area was normalized by that of PA-labeled glucose hexamer (2 pmol/area) in PA-glucose oligomer standard (degree of polymerization 3–15, TaKaRa, Kyoto, Japan). The peaks corresponding to Man_{2-5} were measured as the total amount of FOGs through all experiments and normalized by 1.0 OD_{600} unit of cells (~2.0 × 10^7 cells).

MALDI-TOF MS analysis

MALDI-TOF MS analyses were carried out on an AXIMA-QIT instrument (Shimadzu, Kyoto, Japan) using 2,5-dihydroxybenzoic acid (Shimadzu, Kyoto, Japan) as the matrix as described previously (42).

Quantitative analysis of nucleotide sugars

The preparation and ion-pair reversed-phase HPLC of the nucleotide sugars were carried out as described previously (43). Each of the peaks derived from UDP-Glc, UDP-GlcNAc, and GDP-Man was assigned by comparing its elution position with that of standards (Sigma-Aldrich).

Protein extraction and immunoblot analysis

For immunoblot analysis, cells were grown in appropriate media overnight. After the saturated cells were re-inoculated into fresh media, they were grown to the mid-log phase. Five OD_{600} units of cells were collected and washed with distilled water. Whole protein was extracted by treating cell pellets with 50 μl of 200 mM NaOH for 20 min on ice, after which 50 μl of 2× sample buffer (0.25 M Tris-HCl (pH 6.8), 8% SDS, 40% glycerol, 0.02% bromphenol blue, and 0.4 M DTT) was added, and the samples were boiled for 5 min. Aliquots of 5 μl of the supernatant were subjected to SDS-PAGE analysis. The separated proteins were transferred to a polyvinylidene difluoride membrane, and the membrane was blocked with TTBS (25 mM Tris-HCl (pH 7.4), 150 mM NaCl, and 0.1% (v/v) Tween 20) containing 0.5% (w/v) skim milk. The blot was incubated with F-7, an anti-HA mouse mAb (for detection of Wsc1-HA; 1:10,000; Santa Cruz Biotechnology, Inc., Dallas, TX), an anti-phospho-p44/42 MAPK polyclonal rabbit antibody (for detection of phosphorylated Mpk1; 1:5000; Cell Signaling Technology Japan, (Tokyo, Japan)) or an anti-Pgk1 mouse mAb,22C5 (1:10,000; Thermo Fisher Scientific), followed by incubation with a horseradish peroxidase–conjugated anti-mouse IgG antibody (1:5000; GE Healthcare) or a horseradish peroxidase–conjugated anti-rabbit IgG antibody (1:5000; GE Healthcare), both in TTBS containing 0.5% (w/v) skim milk. Bands were visualized using a LAS3000 Mini system (Fujifilm Co., Tokyo, Japan) using Immobilon Western reagents (Millipore).

RNA-Seq

Yeast cells were harvested using membrane filters (mixed cellulose esters, 0.45 μm, Merck) and directly transferred into liquid nitrogen. Frozen cells were mixed with frozen droplets of 600 μl of lysis buffer (20 mM Tris-HCl (pH 7.5), 150 mM NaCl, 5 mM $MgCl_2$, 1 mM DTT, 100 μg/ml cycloheximide, and 1% Triton X-100) and lysed by a multi-bead shocker (Yasui Kikai). Lysates were treated with 25 units of TURBO DNase (Thermo Fisher Scientific) and cleared by centrifugation at 20,000 $\times$ *g* for 10 min at 4 °C. TRIzol LS reagent (Thermo Fisher Scientific) and the Direct-zol RNA kit (Zymo Research, Irvine, CA) were used for the extraction of total RNA. Ribosomal RNAs were depleted using the Ribo-Zero Gold rRNA removal kit (yeast) (Illumina, San Diego, CA), and preparation of the RNA-Seq library was performed using the TruSeq Stranded mRNA Library Prep Kit (Illumina) following the manufacturer's instructions.

The libraries were sequenced on a HiSeq 4000 system (Illumina). Reads were mapped to yeast transcriptome using TopHat version 2.0.9 (44). We counted the number of reads within the coding sequence for each mRNA and performed the differential expression analysis using the DESeq package (45). The custom R scripts are available upon request.

Author contributions—H. H. and T. S. designed the experiments. H. H., T. M., Y. T., and J. S. performed the HPLC experiments and analyzed the results. R. O. and C. H. analyzed the extracellular/intracellular protein level of Wsc1 by immunoblotting. K. N. analyzed/quantified the intracellular pools of nucleotide sugars. Y. N. performed the study of the localization of FOGs using ManLe-FLAG and analyzed the results. Y. S. and S. I. assisted with RNA-Seq analysis. H. H. wrote the paper with T. S.

Acknowledgments—We are grateful to Professor Sabine Strahl (Heidelberg University) for providing plasmid pRS416-WSC1-HA. We also thank the members of the former Glycometabolome team (RIKEN) for fruitful discussions and Dr. Yoichiro Harada (Kagoshima University) for critical reading of the manuscript. Deep sequencing was performed by the Vincent J. Coates Genomics Sequencing Laboratory at the University of California (Berkeley, CA), supported by National Institutes of Health Instrumentation Grant S10 OD018174. Computations were supported by Manabu Ishii, Itoshi Nikaido, and the Bioinformatics Analysis Environment Service on RIKEN Cloud at RIKEN ACCC.

References

1. Varki, A. (1993) Biological roles of oligosaccharides: all of the theories are correct. *Glycobiology* **3,** 97–130 CrossRef Medline
2. Varki, A. (2017) Biological roles of glycans. *Glycobiology* **27,** 3–49 CrossRef Medline
3. Kornfeld, R., and Kornfeld, S. (1985) Assembly of asparagine-linked oligosaccharides. *Annu. Rev. Biochem.* **54,** 631–664 CrossRef Medline
4. Lehle, L., Strahl, S., and Tanner, W. (2006) Protein glycosylation, conserved from yeast to man: a model organism helps elucidate congenital human diseases. *Angew. Chem. Int. Ed. Engl.* **45,** 6802–6818 CrossRef Medline
5. Xu, C., and Ng, D. T. (2015) Glycosylation-directed quality control of protein folding. *Nat. Rev. Mol. Cell Biol.* **16,** 742–752 CrossRef Medline
6. Vembar, S. S., and Brodsky, J. L. (2008) One step at a time: endoplasmic reticulum-associated degradation. *Nat. Rev. Mol. Cell Biol.* **9,** 944–957 CrossRef Medline
7. Helenius, A., and Aebi, M. (2004) Roles of *N*-linked glycans in the endoplasmic reticulum. *Annu. Rev. Biochem.* **73,** 1019–1049 CrossRef Medline
8. Caramelo, J. J., and Parodi, A. J. (2008) Getting in and out from calnexin/calreticulin cycles. *J. Biol. Chem.* **283,** 10221–10225 CrossRef Medline
9. Lesage, G., and Bussey, H. (2006) Cell wall assembly in *Saccharomyces cerevisiae*. *Microbiol. Mol. Biol. Rev.* **70,** 317–343 CrossRef Medline
10. Orlean, P. (2012) Architecture and biosynthesis of the *Saccharomyces cerevisiae* cell wall. *Genetics* **192,** 775–818 CrossRef Medline
11. Gentzsch, M., and Tanner, W. (1996) The PMT gene family: protein *O*-glycosylation in *Saccharomyces cerevisiae* is vital. *EMBO J.* **15,** 5752–5759 CrossRef Medline
12. Hill, K., Boone, C., Goebl, M., Puccia, R., Sdicu, A. M., and Bussey, H. (1992) Yeast KRE2 defines a new gene family encoding probable secretory proteins, and is required for the correct *N*-glycosylation of proteins. *Genetics* **130,** 273–283 Medline
13. Nakatsukasa, K., Okada, S., Umebayashi, K., Fukuda, R., Nishikawa, S., and Endo, T. (2004) Roles of *O*-mannosylation of aberrant proteins in reduction of the load for endoplasmic reticulum chaperones in yeast. *J. Biol. Chem.* **279,** 49762–49772 CrossRef Medline
14. Hirayama, H., Fujita, M., Yoko-o, T., and Jigami, Y. (2008) *O*-Mannosylation is required for degradation of the endoplasmic reticulum-associated degradation substrate Gas1*p via the ubiquitin/proteasome pathway in *Saccharomyces cerevisiae*. *J. Biochem.* **143,** 555–567 CrossRef Medline
15. Goder, V., and Melero, A. (2011) Protein *O*-mannosyltransferases participate in ER protein quality control. *J. Cell Sci.* **124,** 144–153 CrossRef Medline
16. Xu, C., Wang, S., Thibault, G., and Ng, D. T. (2013) Futile protein folding cycles in the ER are terminated by the unfolded protein *O*-mannosylation pathway. *Science* **340,** 978–981 CrossRef Medline
17. Hirayama, H., Hosomi, A., and Suzuki, T. (2015) Physiological and molecular functions of the cytosolic peptide:*N*-glycanase. *Semin. Cell Dev. Biol.* **41,** 110–120 CrossRef Medline
18. Harada, Y., Hirayama, H., and Suzuki, T. (2015) Generation and degradation of free asparagine-linked glycans. *Cell Mol. Life Sci.* **72,** 2509–2533 CrossRef Medline
19. Suzuki, T., and Funakoshi, Y. (2006) Free *N*-linked oligosaccharide chains: formation and degradation. *Glycoconj. J.* **23,** 291–302 CrossRef Medline
20. Harada, Y., Masahara-Negishi, Y., and Suzuki, T. (2015) Cytosolic-free oligosaccharides are predominantly generated by the degradation of dolichol-linked oligosaccharides in mammalian cells. *Glycobiology* **25,** 1196–1205 CrossRef Medline
21. Harada, Y., Buser, R., Ngwa, E. M., Hirayama, H., Aebi, M., and Suzuki, T. (2013) Eukaryotic oligosaccharyltransferase generates free oligosaccharides during *N*-glycosylation. *J. Biol. Chem.* **288,** 32673–32684 CrossRef Medline
22. Hirayama, H., and Suzuki, T. (2011) Metabolism of free oligosaccharides is facilitated in the och1Δ mutant of *Saccharomyces cerevisiae*. *Glycobiology* **21,** 1341–1348 CrossRef Medline
23. Suzuki, T., Kitajima, K., Emori, Y., Inoue, Y., and Inoue, S. (1997) Site-specific de-*N*-glycosylation of diglycosylated ovalbumin in hen oviduct by endogenous peptide:*N*-glycanase as a quality control system for newly synthesized proteins. *Proc. Natl. Acad. Sci. U.S.A.* **94,** 6244–6249 CrossRef Medline
24. Hirsch, C., Blom, D., and Ploegh, H. L. (2003) A role for *N*-glycanase in the cytosolic turnover of glycoproteins. *EMBO J.* **22,** 1036–1046 CrossRef Medline
25. Hirayama, H., Seino, J., Kitajima, T., Jigami, Y., and Suzuki, T. (2010) Free oligosaccharides to monitor glycoprotein endoplasmic reticulum-associated degradation in *Saccharomyces cerevisiae*. *J. Biol. Chem.* **285,** 12390–12404 CrossRef Medline
26. Chantret, I., and Moore, S. E. (2008) Free oligosaccharide regulation during mammalian protein *N*-glycosylation. *Glycobiology* **18,** 210–224 CrossRef Medline
27. Hossain, T. J., Hirayama, H., Harada, Y., and Suzuki, T. (2016) Lack of the evidence for the enzymatic catabolism of Man1GlcNAc2 in *Saccharomyces cerevisiae*. *Biosci. Biotechnol. Biochem.* **80,** 152–157 CrossRef Medline
28. Umekawa, M., Ujihara, M., Makishima, K., Yamamoto, S., Takematsu, H., and Wakayama, M. (2016) The signaling pathways underlying starvation-

induced upregulation of α-mannosidase Ams1 in *Saccharomyces cerevisiae*. *Biochim. Biophys. Acta* **1860,** 1192–1201 CrossRef Medline
29. Chantret, I., Frénoy, J. P., and Moore, S. E. (2003) Free-oligosaccharide control in the yeast *Saccharomyces cerevisiae*: roles for peptide:*N*-glycanase (Png1p) and vacuolar mannosidase (Ams1p). *Biochem. J.* **373,** 901–908 CrossRef Medline
30. Hossain, M. A., Nakano, R., Nakamura, K., Hossain, M. T., and Kimura, Y. (2010) Molecular characterization of plant acidic α-mannosidase, a member of glycosylhydrolase family 38, involved in the turnover of *N*-glycans during tomato fruit ripening. *J. Biochem.* **148,** 603–616 CrossRef Medline
31. Lodder, A. L., Lee, T. K., and Ballester, R. (1999) Characterization of the Wsc1 protein, a putative receptor in the stress response of *Saccharomyces cerevisiae*. *Genetics* **152,** 1487–1499 Medline
32. Dwivedi, R., Nothaft, H., Reiz, B., Whittal, R. M., and Szymanski, C. M. (2013) Generation of free oligosaccharides from bacterial protein *N*-linked glycosylation systems. *Biopolymers* **99,** 772–783 CrossRef Medline
33. Iwatsuka, K., Watanabe, S., Kinoshita, M., Kamisue, K., Yamada, K., Hayakawa, T., Suzuki, T., and Kakehi, K. (2013) Free glycans derived from glycoproteins present in human sera. *J. Chromatogr. B Analyt. Technol. Biomed. Life Sci.* **928,** 16–21 CrossRef Medline
34. Suzuki, T., Matsuo, I., Totani, K., Funayama, S., Seino, J., Taniguchi, N., Ito, Y., and Hase, S. (2008) Dual-gradient high-performance liquid chromatography for identification of cytosolic high-mannose-type free glycans. *Anal. Biochem.* **381,** 224–232 CrossRef Medline
35. Hanlon, S. E., Rizzo, J. M., Tatomer, D. C., Lieb, J. D., and Buck, M. J. (2011) The stress response factors Yap6, Cin5, Phd1, and Skn7 direct targeting of the conserved co-repressor Tup1-Ssn6 in *S. cerevisiae*. *PLoS One* **6,** e19060 CrossRef Medline
36. Patel, B. K., Gavin-Smyth, J., and Liebman, S. W. (2009) The yeast global transcriptional co-repressor protein Cyc8 can propagate as a prion. *Nat. Cell Biol.* **11,** 344–349 CrossRef Medline
37. Lommel, M., Bagnat, M., and Strahl, S. (2004) Aberrant processing of the WSC family and Mid2p cell surface sensors results in cell death of *Saccharomyces cerevisiae O*-mannosylation mutants. *Mol. Cell. Biol.* **24,** 46–57 CrossRef Medline
38. Longtine, M. S., McKenzie, A., 3rd, Demarini, D. J., Shah, N. G., Wach, A., Brachat, A., Philippsen, P., and Pringle, J. R. (1998) Additional modules for versatile and economical PCR-based gene deletion and modification in *Saccharomyces cerevisiae*. *Yeast* **14,** 953–961 CrossRef Medline
39. Gietz, R. D. (2014) Yeast transformation by the LiAc/SS carrier DNA/PEG method. *Methods Mol. Biol.* **1205,** 1–12 CrossRef Medline
40. Nakanishi-Shindo, Y., Nakayama, K., Tanaka, A., Toda, Y., and Jigami, Y. (1993) Structure of the *N*-linked oligosaccharides that show the complete loss of α-1,6-polymannose outer chain from och1, och1 mnn1, and och1 mnn1 alg3 mutants of *Saccharomyces cerevisiae*. *J. Biol. Chem.* **268,** 26338–26345 Medline
41. Ohashi, T., and Takegawa, K. (2010) *N*- and *O*-linked oligosaccharides completely lack galactose residues in the gms1och1 mutant of *Schizosaccharomyces pombe*. *Appl. Microbiol. Biotechnol.* **86,** 263–272 CrossRef Medline
42. Suzuki, T., Hara, I., Nakano, M., Shigeta, M., Nakagawa, T., Kondo, A., Funakoshi, Y., and Taniguchi, N. (2006) Man2C1, an α-mannosidase, is involved in the trimming of free oligosaccharides in the cytosol. *Biochem. J.* **400,** 33–41 CrossRef Medline
43. Nakajima, K., Kitazume, S., Angata, T., Fujinawa, R., Ohtsubo, K., Miyoshi, E., and Taniguchi, N. (2010) Simultaneous determination of nucleotide sugars with ion-pair reversed-phase HPLC. *Glycobiology* **20,** 865–871 CrossRef Medline
44. Trapnell, C., Pachter, L., and Salzberg, S. L. (2009) TopHat: discovering splice junctions with RNA-Seq. *Bioinformatics* **25,** 1105–1111 CrossRef Medline
45. Anders, S., and Huber, W. (2010) Differential expression analysis for sequence count data. *Genome Biol.* **11,** R106 CrossRef Medline